Incorporating interpretation uncertainties from deterministic 3D hydrostratigraphic models in groundwater models

Trine Enemark[1], Rasmus Bødker Madsen[2], Torben O. Sonnenborg[3], Lærke Therese Andersen[2], Peter B.E. Sandersen[2], Jacob Kidmose[3], Ingelise Møller[2], Thomas Mejer Hansen[4], Karsten Høgh Jensen[1] and Anne-Sophie Høyer[2]

[1]Department of Geosciences and Natural Resource Management, University of Copenhagen, Copenhagen, 1350, Denmark
[2]Geological Survey of Denmark and Greenland, Near-surface Land- and Marine geology, Aarhus, 8000, Denmark
[3]Geological Survey of Denmark and Greenland, Hydrology, Copenhagen, 1350, Denmark
[4]Department of Geoscience, University of Aarhus, Aarhus, 8000, Denmark

10   *Correspondence to*: Trine Enemark (tre@ign.ku.dk)

Abstract. Many 3D hydrostratigraphic models of the subsurface are interpreted as deterministic models, where an experienced modeler combines relevant geophysical and geological information with background geological knowledge. Depending on the quality of the information from the input data, the interpretation phase will typically be accompanied by an estimated qualitative interpretation uncertainty. Given the qualitative nature of uncertainty, it is difficult to propagate the uncertainty to groundwater models. In this study, a stochastic simulation-based methodology to characterize interpretation uncertainty within a manual interpretation-based layer model is applied in a groundwater modeling setting. Three levels of interpretation uncertainty scenarios are generated and three locations in the models representing different geological structures are analyzed. The impact of interpretation uncertainty on predictions of capture zone area and median travel time is compared to the impact of parameter uncertainty in the groundwater model. The main result is that in areas with thick and large aquifers and low geological uncertainty, the impact of interpretation uncertainty is negligible compared to the hydrogeological parameterization, while it may introduce a significant contribution in areas with thinner and smaller aquifers with high geologic uncertainty. The influence of the interpretation uncertainties is thus dependent on the geological setting as well as the confidence of the interpreter. In areas with thick aquifers, this study confirms existing evidence that if the conceptual model is well-defined, interpretation uncertainties within the conceptual model have limited impact on groundwater model predictions.

1 Introduction

Hydrostratigraphic models are the backbone of a groundwater model. They define the physical structure and the parameter zonation according to which movement of water, storage and solute transport takes place in the groundwater model. The hydrostratigraphic model is subject to uncertainty, and it is well known that it forms a large source of uncertainty in the groundwater model predictions (e.g. Huysmans and Dassargues, 2009; Moore and Doherty, 2005; Troldborg et al., 2007; Poeter and Anderson, 2005). Characterizing these uncertainties is important as it can provide decision-makers with information about the accuracy of model predictions and has been the subject of numerous studies (e.g. Barfod et al., 2018; Feyen and Caers, 2006; Li et al., 2016; Zhang et al., 2021).

Generally, hydrostratigraphic modeling can be divided into two main groups, in which uncertainties are characterized differently: The interpretation-based approaches and the geostatistical approaches. In the interpretation-based approaches, a single deterministic geological or hydrostratigraphic model is constructed manually through the modeler's co-interpretation of all available data (e.g. Høyer et al., 2015; Jørgensen et al., 2013; Royse, 2010). The resulting model is viewed as the "best possible" representation of the subsurface, given the available data and information. The main advantage is that they are directly based on expert knowledge, thereby ensuring geological realism. This has traditionally been the favored method for producing geological models. However, a common criticism is that both the final hydrostratigraphic model and the interpretation uncertainties are inherently subjective and biased in nature (Wellmann and Caumon, 2018). In contrast, it has also been argued that given a proper description of the subjective information, the subjective element becomes a strength rather than a weakness (Curtis, 2012).

In geostatistical simulation approaches, multiple realizations are generated in order to represent a span of "equally possible" models of the subsurface (e.g. Høyer et al., 2017; Madsen et al., 2021a; Mariethoz and Caers, 2015; Stafleu et al., 2011) and hereby account for the inherent uncertainty of the geological model. Based on a set of assumptions, the equally possible models are generated automatically representing the unstructured uncertainty within the conceptual model. Geostatistical simulations have been used in a number of studies to analyze the effects of combined geological and parameter uncertainty in relation to groundwater modelling (e.g. He et al., 2013; Refsgaard et al., 2012), just like other studies focus on how the groundwater modelling can be optimized when simulating both hydrostratigraphic units and hydraulic conductivity uncertainty (e.g. Benoit et al., 2021). As the uncertainty modelling is already well-established and a more natural consequence of geostatistical modeling, this paper aims at addressing the issue that the interpretation models lack a clear way to characterize uncertainties quantitatively.

In the interpretation-based geological models, a qualitative measure of uncertainty may be assigned to each interpretation point by the modeler. These uncertainties are based on several factors related both to the geological interpretation and the data (data type, - resolution, - density and – quality) (Høyer et al., 2023; Sandersen et al., 2018). Due to the qualitative and subjective nature of the uncertainty measure related to the perceived uncertainty of the geologist while producing the deterministic interpretation model, this information has previously been lost and hence, not incorporated in subsequent modelling, as groundwater modelling. Thus, the uncertainties have only been discussed qualitatively when the purpose of the models required it, for instance in relation to landfill leachate risk assessment (Høyer et al., 2019) or groundwater vulnerability mapping (Hansen et al., 2016; Sandersen, 2008).

One attempt to consider the uncertainties of the manual interpretation models focus on the uncertainties related to the difference in conceptual geological understanding between different modelers. To consider this, some studies have engaged multiple teams of geological modelers to interpret the same data with an unknown conceptual model to come up with what they believe is the most likely model (e.g. Harrar et al., 2003; Hills and Wierenga, 1994; Refsgaard et al., 2006; Seifert et al., 2012). This approach is not widely applied as it is labor-intensive, and it is difficult to analyze the resulting uncertainty captured through the multiple models.

However, recently approaches have been developed that transform the qualitative uncertainties of an interpretation-based hydrostratigraphic model to an ensemble of different realizations of the subsurface configuration through geostatistical simulation. In Troldborg et al. (2021), borehole interpretations were perturbed by assuming a normal distribution with a standard deviation reflecting a predefined group-wise uncertainty. Different sequential gaussian simulation (SGS) realizations were generated by conditioning them on different perturbed borehole interpretations. The realizations were applied in an impact assessment of sheet piles on the water table. Further, Madsen et al. (2022) presented the geology-driven modeling approach where a deterministic interpretation-based hydrostratigraphic model can be transformed into a set of hydrostratigraphic realizations through SGS and interpretation uncertainties defined by the interpreter. The underlying probability distributions used in the SGS are inferred using a likelihood function, as opposed to the variogram-based modelling of Troldborg et al. (2021), which enables correlated effects of the interpretation uncertainty to be considered.

In this study, the method of Madsen et al., (2022) is implemented in a groundwater modeling context for an area in central Denmark, where the interpretation-based hydrostratigraphic model is based on information from boreholes, airborne electromagnetic data and geoelectrical data (Enemark et al., 2022; Madsen et al., 2022). To our knowledge, the interpretation uncertainty for all layer boundaries in a manual, interpretation-based model has never been analyzed systematically in a groundwater model. Specifically, the influence of interpretation uncertainty on groundwater model predictions is evaluated in terms of the extent of the capture zones and the median travel times of water. The investigation is performed for three well fields in the study area that represent different geological structures and different levels of uncertainty. Three scenarios of

diverse levels of uncertainty are investigated ranging from the overconfident interpreter to the cautious one. Overconfident interpreters will generally assign low uncertainties to their interpretations while the opposite is the case for cautious interpreters. Because the resulting groundwater models are affected by uncertainties in both the hydrostratigraphic and hydrological domain, the overall effect and significance of propagating the interpretation uncertainties are compared to uncertainties in the parameters of the groundwater model, such as hydraulic conductivity.

2 Study area

2.1 Hydrological and geological setting

The study area covers 127 km² and is located just north of Horsens Fjord in Jutland, Denmark (Figure 1). The catchment is delineated by the topography that ranges from 170 m above sea level (a.s.l.) in the north to 0 m a.s.l. at the fjord. Approximately 2.7 M m³/year of groundwater is abstracted for drinking water from 20 different well fields within the study area. The groundwater system is restricted to the geological succession above the Paleogene clay, which is assumed to be impermeable and has a large thickness apart from areas where deep buried valleys are eroded into the Paleogene clay. In parts of the model area, erosional remnants of Miocene sand, silt and clay exist on the plateaus, although the Paleogene clay is directly overlaid by Quaternary deposits in most of the area. The Quaternary succession is influenced by glacial erosion and both glaciotectonics and multiple cross-cutting buried valleys have previously been mapped (Figure 1; Jørgensen et al., 2010; Sandersen and Jørgensen, 2016). The Quaternary deposits consist of glacial and interglacial deposits of till, meltwater clay and sand, freshwater clay, sand and gyttja.

A deterministic and manually interpreted hydrostratigraphic model has been constructed for the area (Andersen and Sandersen, 2020) following the national guidelines described in Sandersen et al. (2018). The manual modelling is performed in the geological modelling software Geoscene3D (I-GIS, 2023) along a grid of fixed interpretation profiles placed such that they cross important geological structures and data. Three of these interpretation profiles are shown in Figure 2. The figure shows the interpretation points together with the gridded layer surfaces and borehole data within a buffer of 50 m of the profile. Each of the layers in the manual model is constituted by a top and a bottom 2D surface.

Interpretation points were manually placed along the interpretation profiles. The aim was an even spacing of a few hundred meters between points, with a closer spacing in areas with marked variations. Subsequently, the layers are interpolated using kriging with adjusted semivariograms dedicated to each surface. To ensure that surfaces do not cross, they are adjusted using a dedicated tool in the modelling software, after the gridding. The modeler sets up rules of succession based on the erosional and depositional setting. Each interpretation point was attributed a qualitative uncertainty measure during the interpretation process, shown with color-coded horizontal ovals in Figure 2. The categories were defined as follows:

Category 1: Most certain interpretation points, typically related to high-quality borehole information.

125 Category 2: Certain interpretation points, based on good quality geophysical data and/or close to borehole data.

Category 3: Intermediate uncertainty, based on geophysical or borehole data of less good quality or ambiguous information.

Category 4: Uncertain information, based on interpretation of data of poor quality, extrapolated data, or no data at all.

130

In the rest of this paper, the deterministic, manually generated, interpretation-based layer hydrostratigraphic model (Andersen and Sandersen, 2020) will be referred to as the Manual Interpretation model.

The Manual Interpretation model covers five pre-Quaternary layers and nine Quaternary layers. The pre-Quaternary layers
135 consist of limestone, Paleogene clay, lower Miocene clay, Miocene sand, and upper Miocene clay. The Quaternary layers are divided into alternating clay and sand layers. The lowermost Quaternary layers are exclusively interpreted as valley infill deposits whereas the upper Quaternary layers exist throughout the model area. The hydrostratigraphic model was constructed to focus on the hydrological properties of the deposits and do not distinguish between lithologies deposited in different geological environments, such as meltwater clay and clay till deposits.
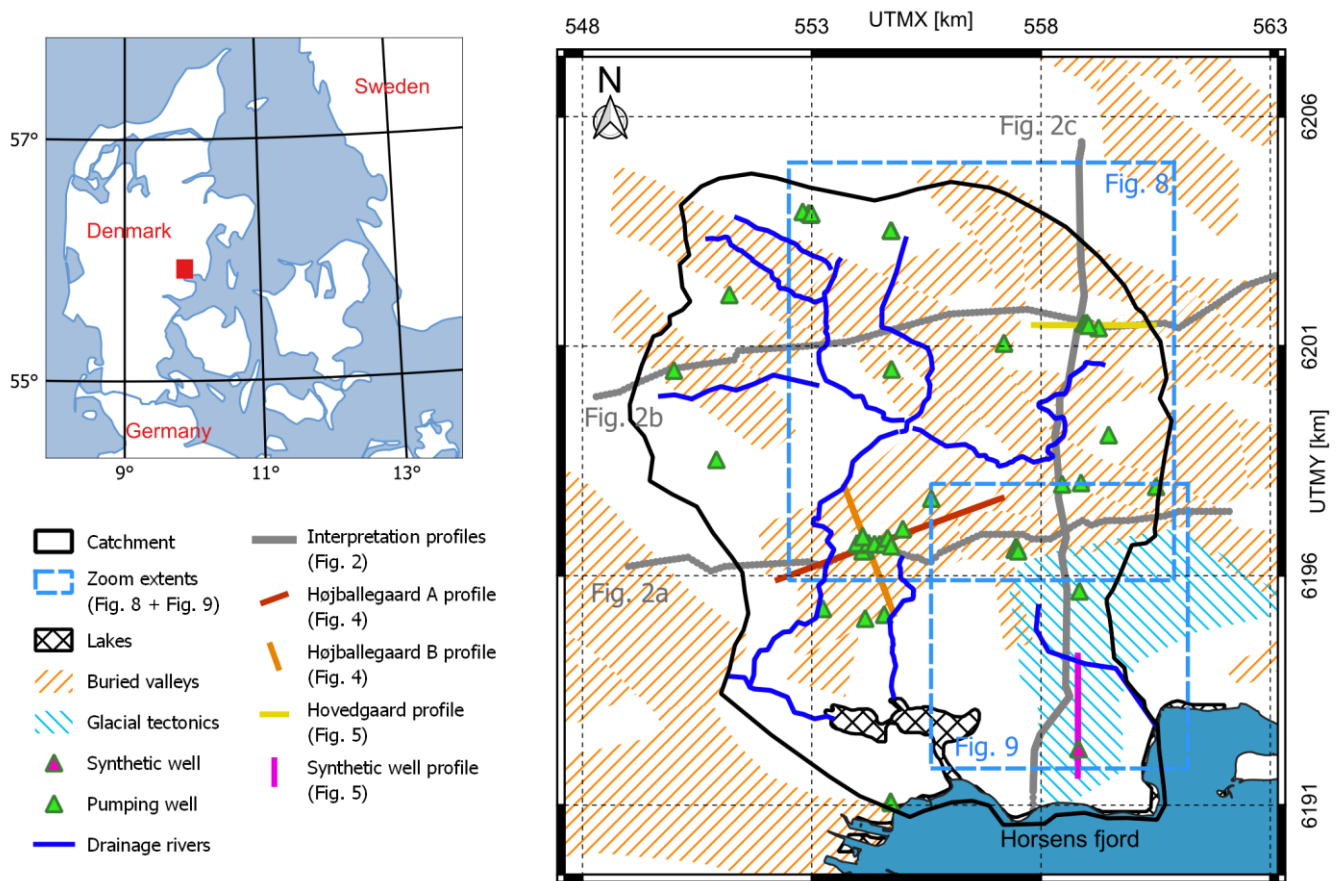
Figure 1: Location of the catchment, water abstraction wells, main rivers, glacial tectonics, buried valleys, profiles shown in Figures 2, 4 and 5, areas and zoom extents used in Figure 9 and Figure 10, respectively.

2.2 Selected investigation sites

The study is concentrated around two well fields in the area, Højballegård and Hovedgård, and a synthetic well field (see Figure 1). The two real well fields (Højballegård and Hovedgård) were chosen because they represent different geological structures from which water is abstracted. The synthetic well field does not exist in the real world but was introduced in the analysis to represent an area with low data availability and thus a higher level of geological uncertainty. In the following, the geology and hydrostratigraphy of the three areas are summarized based on details described in previous studies (Andersen and Sandersen, 2020; Enemark et al., 2022; Madsen et al., 2022).

2.2.1 Højballegård well field

Højballegård well field with 17 abstraction wells is situated in the central part of the catchment (Figure 1) and is the largest well field in the area, responsible for 87 % of the groundwater abstraction The water is abstracted from a deep SW-NE oriented

buried valley structure that shows widths up to 2 km and depths up to 220 m. According to the borehole information, the valley infill deposits are relatively complex with varying deposits of glacial origin including meltwater sand, meltwater clay and clay

155   till as well as thick occurrences of interglacial clay, sand and gyttja. In the Manual Interpretation model (Figure 2a), the valley infill is divided into Quaternary sand and clay. The groundwater at Højballegård is abstracted from two different Quaternary sand layers (see arrows in Figure 2), separated by a clayey aquitard. In the model, the upper abstraction layer groups the meltwater sand deposited as valley infill and the Quaternary sand on the plateaus and can therefore serve as a hydraulic connection between the plateaus and the valley. The layer is laterally extensive (Figure 2a, profile distance 2 – 8.5 km) and

160   has a varying, but usually substantial thickness (around 30 m at the well field). The lower abstraction layer is dedicated valley infill sand and is thus solely present in the buried valleys with a thickness of about 40 m around the well field.
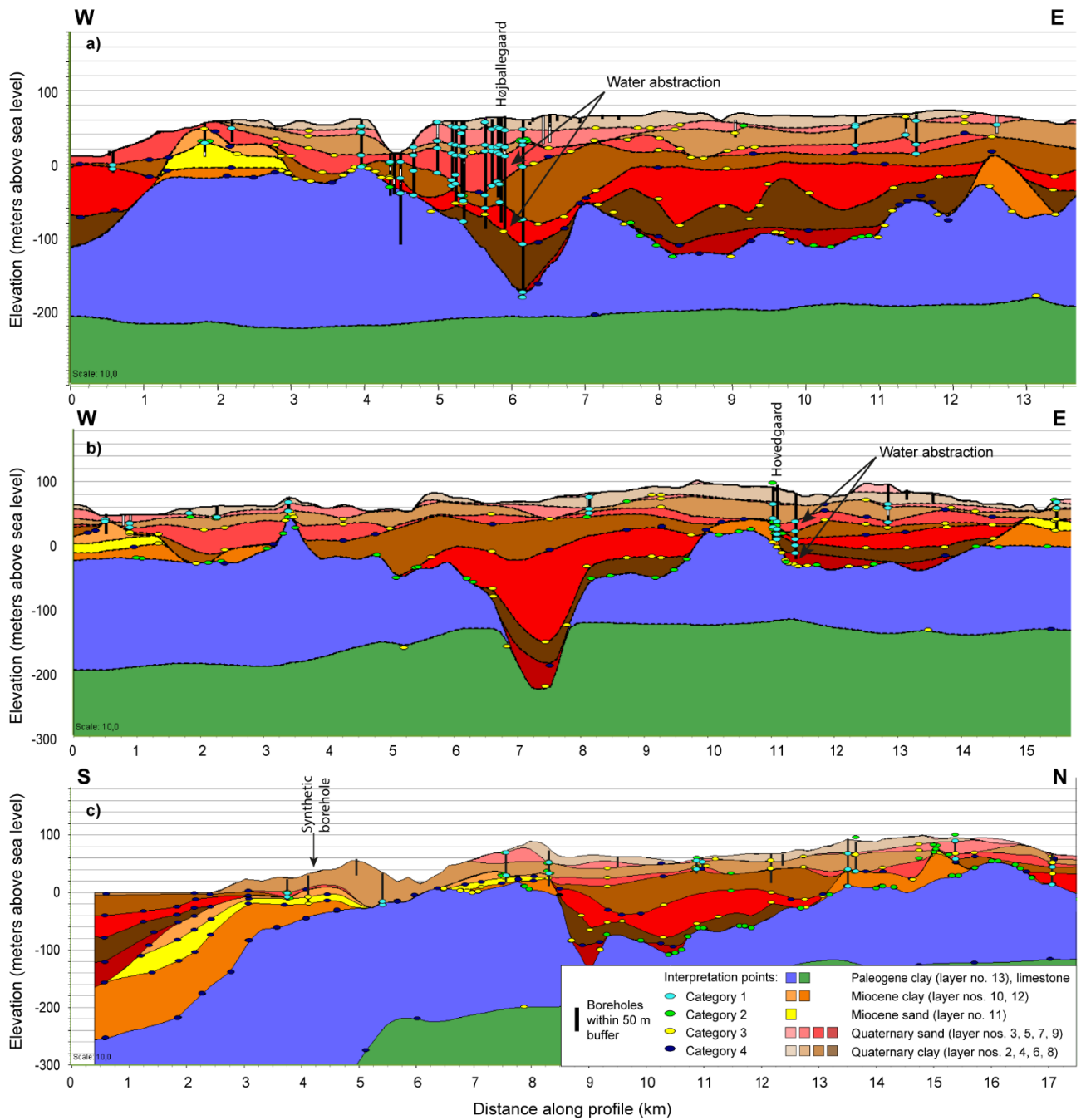
Figure 2: Interpretation profiles through the catchment showing the Manual Interpretation model with interpretation points and their uncertainty categories. Interpretation points and boreholes are shown within a buffer of 50 m from the profile. a) interpretation profile crossing the Højballegård well field, b) interpretation profile crossing Hovedgård well field, c) interpretation profile closest

165

to the synthetic borehole (placed 900 m from the profile). The interpolated position of the borehole is marked at the profile. The locations of the profiles are shown in Figure 1. Vertical exaggeration 10x.

2.2.2 Hovedgård well field

Hovedgård well field is situated in the northeastern part of the catchment (Figure 1) and is a small well field with four wells, responsible for 3% of the water abstraction in the area. The well field is located on the western flank of an SSW-NNE oriented buried valley (Figure 2b). The valley is up to 3 km wide, but only 120 m deep. The valley infill at Hovedgård is less well-described compared to the Højballegård well field, with many lithological descriptions only indicating lithology (sand or clay) rather than depositional environment. According to the Manual Interpretation model (Figure 2b), the valley infill is characterized by thin alternating layers of sand and clay. Water at Hovedgård well field is abstracted from deep sand layers (see arrows in Figure 2), modelled as valley infill. The abstraction layers are therefore restricted to the area of the buried valley and only locally present in the northern and southern parts of the valley.

2.2.3 Synthetic well field

To simulate the response of the models in an area with larger uncertainty, a synthetic well field was included in the southeastern part of the model area with an appropriate distance to the boundaries of the groundwater model (Figure 1). Here, the data is relatively sparse, and the interpretation points are generally assigned high uncertainties. In the groundwater model water is abstracted from the Miocene sand layer and is set to the same rate as for Hovedgård well field. At this location, the Miocene sand is interpreted to be relatively thin (10 m) (Figure 2c). The Miocene layers are interpreted to dip towards south due to the deep-seated fault structure in the southernmost part of the area.

3 Methods

The workflow of the paper is summarized in Figure 3. To evaluate the interpretation uncertainty of an initial interpreted hydrostratigraphic model, the hydrostratigraphic model is perturbed in three different uncertainty scenarios to produce 50 realizations in each scenario. In a groundwater model using the original interpreted hydrostratigraphic model, 200 parameter realizations are selected in a GLUE approach. The 200 behavioral parameter sets are applied using the hydrostratigraphic realizations. In the following, a detailed description of the methodology is provided.
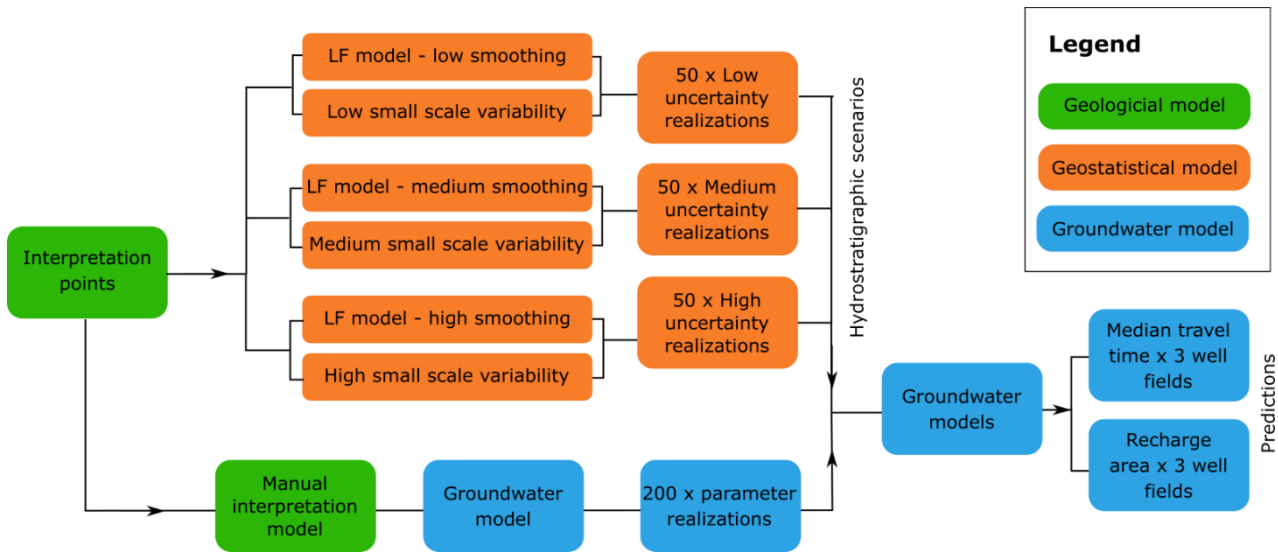
Figure 3: Summary of workflow in the current paper.

3.1 Hydrostratigraphic modeling

The geostatistical modeling described in Madsen et al. (2022; 2021b) is based on the qualitative uncertainties evaluated at each interpretation point during the manually interpreted hydrostratigraphic modeling (Andersen and Sandersen, 2020) (Section 2.1). To apply the methodology, the interpreter must provide; 1) A quantitative estimate of the interpretation point uncertainty based on the qualitatively evaluated uncertainties, and 2) a factor to balance the small-scale variability and large-scale structures (see section 3.1.2). These preparational steps are described in the two following sections.

3.1.1 Point uncertainty estimates

In the applied methodology, each of the qualitative uncertainty categories is quantified using a Gaussian distribution, with the elevation of the interpretation points characterized by a mean and a standard deviation specified by the interpreter. The standard deviation for each uncertainty category is set to increase proportionally with depth and the resolution of the geoelectrical and electromagnetic inversion results. In layers with special properties, where depth cannot be used as a direct proxy for uncertainty, an interpreted value is provided manually based on other information. For instance, the deep-lying Paleogene clay is well-resolved with electromagnetic methods due to its low electrical resistivity, thus having low interpretation uncertainty in the Manual Interpretation model (see e.g. Danielsen et al. (2003)). However, it is essential to note that even with this comparatively low interpretation uncertainty at the well-resolved boundary, the chosen uncertainty level should still reflect the uncertainties related to the processing and inversion of the geophysical data, especially as resolution decreases with depth (Madsen et al., 2022; Viezzoli et al., 2013). Specifically for geoelectrical models, the Depth of Investigation (DOI) can be introduced to help assess the validity of the geophysical model at depth (Christiansen and Auken, 2012). Below the DOI, it is

appropriate to assign a high level of uncertainty even for an apparently well-resolved layer as the deep-lying Paleogene clay. Above the DOI, the quantification of standard deviations should factor in the resolution decrease of the inversion model with depth due to an increasing volume of the subsurface being averaged over and the chosen regularization (Vignoli et al., 2015). Ideally, the standard deviation should also account for the possibility of inversion equivalences related to different parameterization of the inversion scheme (Høyer et al., 2014).

3.1.2 Balancing small-scale variability and large-scale structures

The spatial variability between interpretation points is quantified by extracting 1) the large-scale structures of the interpretation points in a low-frequency (LF)-model and 2) capturing the small-scale variability of the residuals with a Gaussian distribution. As Gaussian simulation rarely leads to realistic geology (Journel and Zhang, 2006), this separation of the point information is introduced in order to improve geological realism in the stochastic hydrostratigraphy by keeping the main geological features intact. In the current setup, the LF-model is obtained by linear interpolation between interpretation points and then applying a smoothing kernel via a sliding window approach on the interpolated grid. To provide a balance between the small-scale variability and large-scale structures, the interpreter must provide a factor ε determining the width of a smoothing kernel used to construct the LF-model. Figure 4 illustrates the structural input provided in the LF-model. In one extreme, the interpretation model is used directly without applying any smoothing (**Error! Reference source not found.**a), giving all structural weight to the interpretation model. In the other extreme, the interpretation model is smoothed such that the LF-content merely becomes the average depth of the layers providing the maximal weight to the small-scale variability (**Error! Reference source not found.**c).

As the significance of geological features vary across the modeling domain, the kernel width ε, and hence level of smoothing, also varies at different locations. The modeler only provides the base level ε and the kernel width is then scaled following a principle of locally assessing the changes in surface elevations. In a layer-based model, significant geological characteristics can correspond to sudden shifts in elevation in the interpretation points. These shifts will not arise through interpolation unless specific interpretation points are strategically positioned to guide the surface behavior accordingly. Thus, sudden shifts in interpretation point elevations are a good proxy for geological features worth extracting in the LF-model. The variance amongst the interpretation points within the sliding window is calculated for the entire surface. If the variance is high, then the modeler has tried to convey large changes in the elevation and the smoothing becomes low to allow the LF-model to follow these structures. In the other case, a low variance of elevation amongst the points within the sliding window leads to more smoothing of the LF-model. In many places with low variance in elevation, high uncertainty is attributed to the interpretation points by the modeler. We attribute this apparent correlation to the fact that a modeler would likely not be willing to make bold structural interpretations in areas where there are no data to support such claims. Thus, the LF-model will indirectly carry less information

in areas with high uncertainty, which is desirable, although the LF-model is based on the spatial structure of the interpretation points and not the uncertainty attributed to them.

245
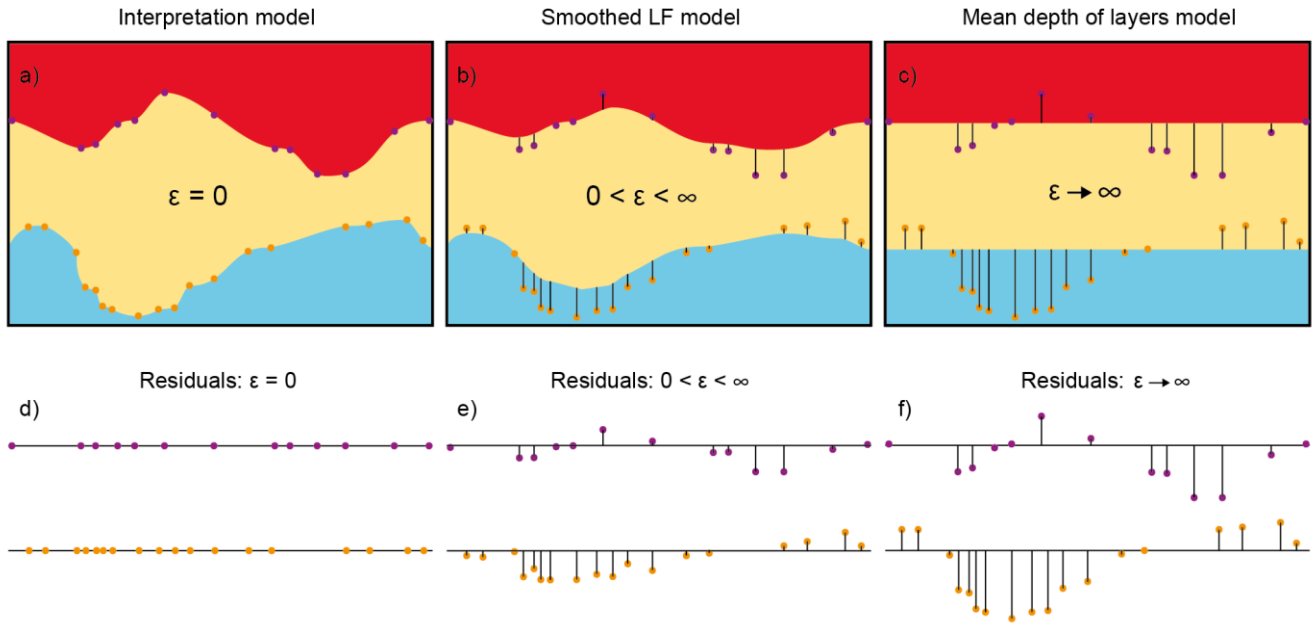
Figure 4: Schematic overview of effect of applying smoothing to a three-layer interpretation model based on interpretation points to obtain the overall structures in a LF model. a) The interpretation model has no smoothing ($\varepsilon = 0$), b) the interpretation model is
250   **smoothed ($0 < \varepsilon < \infty$) and c) the interpretation model is smoothed to a degree that only represents expected average depth of each layer ($\varepsilon \rightarrow \infty$). The resulting residuals for each scenario are shown underneath in d)-f).**

Once a LF-model is established, a statistical model for the small-scale variability is inferred from the residuals, such that a set of realizations of each boundary can be simulated using the quantified spatial variability instead of being interpolated as done
255   in traditional modeling. Ultimately, it is up to the modeler to choose a suitable smoothing that keeps important structural input in the LF-model but allows for the desired spatial variability to be mapped in the residuals (**Error! Reference source not found.**b and **Error! Reference source not found.**e).

3.1.3 Uncertainty scenarios

In this study, three uncertainty scenarios are developed with different point uncertainty quantifications, each consisting of 50 realizations of the subsurface. Furthermore, the Manual Interpretation model does not serve as the ground truth but can be thought of as one possible representation of the subsurface. Thus, the trust in the large-scale structures of the interpretation model is also changed between the three scenarios by varying the applied smoothing factor ε.

First, the uncertainty configuration of Madsen et al. (2022) is adopted as the *"Medium"* uncertainty scenario where $\varepsilon = 700$ m. Second, a *"Low"* uncertainty scenario representing an overconfident interpreter is introduced. To emulate this, all interpretation uncertainties at point scale are reduced by a factor of 3 (compared to Medium scenario) and subsequently the smoothing factor ε is decreased by 500 m to $\varepsilon = 200$ m, thus making the LF-model very similar to the interpretation model. Finally, an insecure interpreter that estimates a *"High"* degree of uncertainty to his/her interpretations is introduced. The standard deviations at point scale of the High scenario are scaled up with a factor of three, while the smoothing factor ε is increased with 500 m to $\varepsilon = 1200$ m to make sure that layers can deviate substantially from the Manual Interpretation model. The standard variation assigned to the different uncertainty scenarios are illustrated in supplementary material S3.

3.2 Groundwater modeling

Applying the same setup as in Enemark et al. (2022), steady-state MODFLOW-NWT (Niswonger et al., 2011) models are developed using the Flopy platform (Bakker et al., 2016). Two outputs of the groundwater model are evaluated: the extent of the capture zones and the median travel times of water particles from the water table to the well screen. These predictions are chosen, as they are not part of the calibration but will be affected by the calibrated parameter zonation. The discretization, boundary conditions and parameterization of the groundwater are described in the following.

3.2.1 Discretization

The horizontal discretization is specified to 100 m by 100 m while the vertical discretization is based on the vertical extent of the hydrostratigraphic units from 165 m a.s.l. to -250 m a.s.l., i.e., each hydrostratigraphic realization has a distinct model grid. By grouping together three plateau sand units, two plateau clay units, two sand units in the buried valleys and two clay units in the buried valleys, the number of hydrostratigraphic units in the groundwater model is eight. The grouped units share the same or similar lithological description in the Manual Interpretation model but differ in their position in the geological sequence. The hydrostratigraphic units are parameterized by horizontal hydraulic conductivity, vertical anisotropy, and porosity.

3.2.2 Boundary conditions

The recharge to the water table is represented as a diffusive source with MODFLOW's recharge (RCH) package as a specified flux distributed over the top of the model. The well abstraction in the model is represented by the specified flux well (WEL)

package. In all models regardless of the geometry of the model grid, the wells are set in the same layer to ensure model predictions can be compared i.e., the depth of the 210 abstraction wells may vary between realizations, but the layer and thereby the lithology will be the same in all models. The lakes and fjord in the southern part of the model area, is represented by the head dependent flux boundary General Head Boundary (GHB) package. To simulate both inflows to streams as well as subsurface tile drains and smaller ditches, the head-dependent flux boundary Drain (DRN) package is applied. The flux to the river cells is used as a calibration target.

3.2.3 Parameterization

Realizations of the parameterization to be used for the individual hydrostratigraphic realizations are generated by Latin Hypercube sampling of parameter values within specified ranges. Five parameters and their prior parameter ranges, which are sampled, are presented in Table 1. A differentiation between buried valley sand and clay and plateau sand and clay is introduced, as the buried valley and plateau sediments may have different hydrogeological properties. Uniform distributions described by a minimum and maximum value are applied, representing prior information on the parameter values. As the sampled parameters are ranging over several orders of magnitude, the sampling was performed from log-uniform distributions. The remaining parameters are not subject to sampling and thus have fixed values as they were shown to be insensitive in initial model runs in the Manual Interpretation model.

To obtain a range of posterior parameter sets, a generalized likelihood uncertainty estimation (GLUE) approach (Beven and Binley, 1992) is applied. Applying this approach, a subset of parameter sets that satisfy a set of predefined constraints simultaneously is obtained. Using the Manual Interpretation model, 10,000 realizations are run based on the prior parameter ranges presented in Table 1. Of these simulations, 200 parameter sets are retained according to the criteria below. Initial model runs in the Manual Interpretation model showed that the predictions of interest, capture zone area and travel time, do not change significantly after 200 model runs (supplementary material S1). Threshold on selected performance metrics is applied based on values in the Danish groundwater modeling guideline (Henriksen et al., 2017). The following thresholds are applied: 0.9 m on the mean error of hydraulic heads, 5 % on the river observation error and 9 m on the root mean square error of hydraulic heads. Initial model runs showed that the same parameter values in different uncertainty scenarios attained similar performance. Therefore, these parameter sets have then been applied to the other uncertainty scenarios. The posterior parameter distributions are presented in supplementary material S2.

Table 1: Parameter value ranges and distributions used in the Manual Interpretation groundwater models. Kh refers to horizontal hydraulic conductivity, while cond refers to conductance.

Parameter	Alias	Sampling/ Fixed	Minimum	Maximum	Unit
Kh Quaternary Plateau sand	Kh QPS	Sampling	1	100	m/d

Kh Quaternary Plateau clay	Kh QPC	Sampling	0.01	2	m/d
Kh Quaternary Valley sand	Kh QVS	Sampling	1	100	m/d
Kh Quaternary Valley clay	Kh QVC	Sampling	0.01	2	m/d
Kh Miocene sand	Kh MS	Sampling	1	100	m/d
Kh Miocene clay	-	Fixed	0.01		m/d
Kh Paleogene clay	-	Fixed	0.01		m/d
Kh Limestone	-	Fixed	1		m/d
Drain cond	-	Fixed	0.05		m^2/d
General Head Boundary cond	-	Fixed	0.05		m^2/d
River cond	-	Fixed	5		m^2/d
Vertical anisotropy	-	Fixed	3		-
Porosity	-	Fixed	0.3		-

3.2.4 Particle tracking

Particle tracking simulations are performed using MODPATH 6 (Pollock 2012). In each topmost active cells, 10 particles are tracked forward to discharge points and the particles discharging to the well fields of interest (Section 2.2) are extracted. Initial

320 simulations in Enemark et al. (2022) showed that the capture zone area stabilizes when around 10 particles are inserted in the upper cells of the layer model in a layer grid. Only particles with a travel time of less than 200 years are retained, as 200 years is the typical value for determining capture zone areas in Denmark (Iversen et al., 2009).

4 Results

4.1 Hydrostratigraphic model

325 The quantified boundary uncertainties are illustrated in four cross sections around the three well fields (Figure 5 and Figure 6). The topmost profiles (Figure 5a,e and Figure 6a,e) show the cross sections through the Manual Interpretation model. The three profiles below illustrate the boundary uncertainties in the Low, Medium and High uncertainty scenario in terms of mode and entropy. The mode represents the most probable value, while entropy is a measure of the uncertainty associated with the mode. In Figure 5 and Figure 6, the mode is represented by the boundaries where the color changes and the entropy is

330 superimposed such that the colors become increasingly transparent when the entropy is high (i.e., uncertainty is high) and conversely has the true color when the entropy is zero. The large difference in the interpretation uncertainty in the three

uncertainty scenarios is overall manifested as increasingly thicker zones of uncertainty around the boundaries going from the Low over the Medium to the High uncertainty scenario (e.g., black ellipsis Figure 6b-d). The overall conceptual model consists of a thick base of impermeable Paleogene clay and alternating layers of Quaternary clay and sand situated on top and is preserved in all scenarios. If either of these mode models were presented as a sole model to be used for groundwater modeling, it would be hard to dismiss to be any less true or useful than the Manual Interpretation model. Thus, the important overall structures carried over from the LF-model are considered a fair representation of the overall geology, while the interpretation uncertainty at the boundaries is showcased by entropy.

345
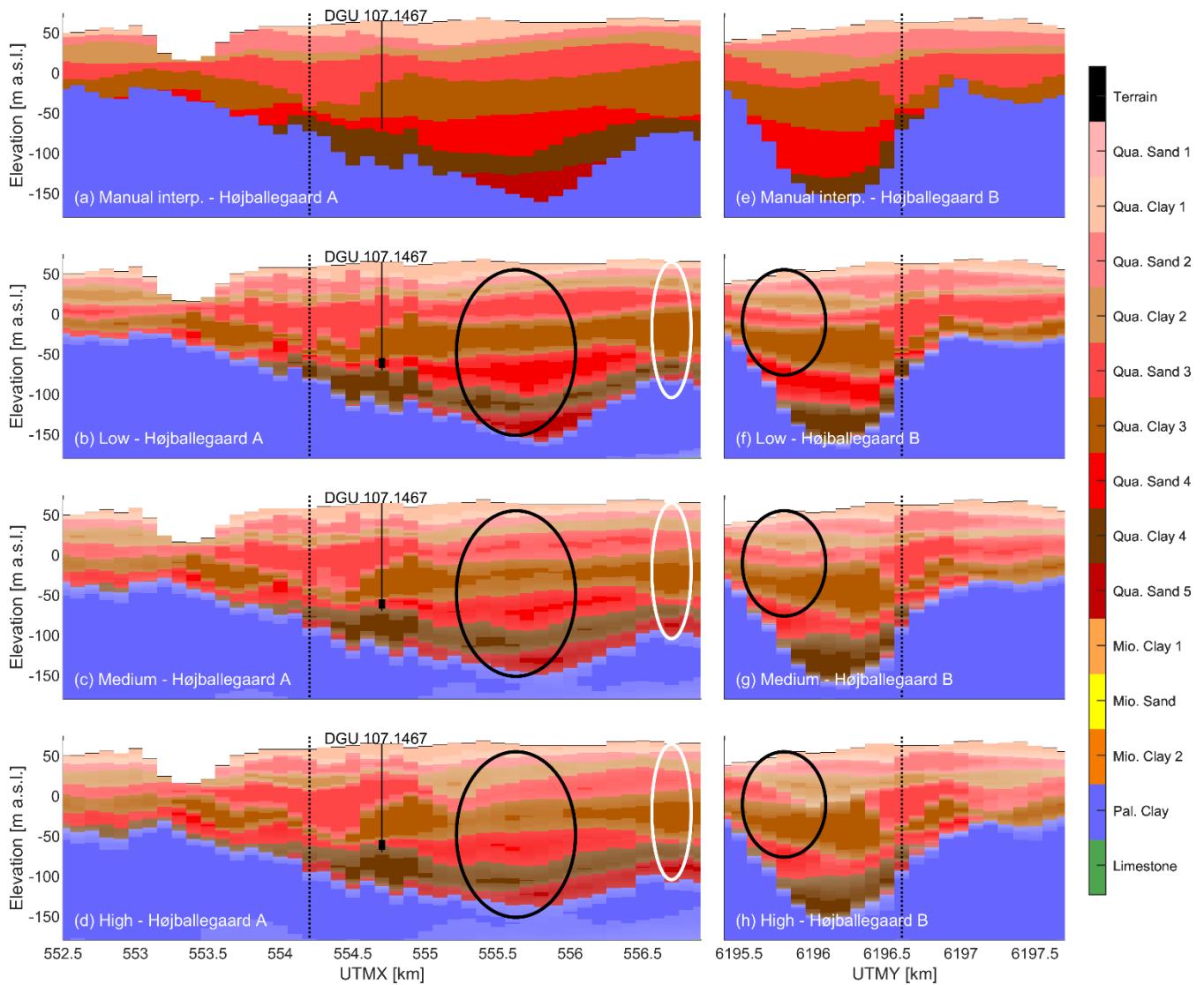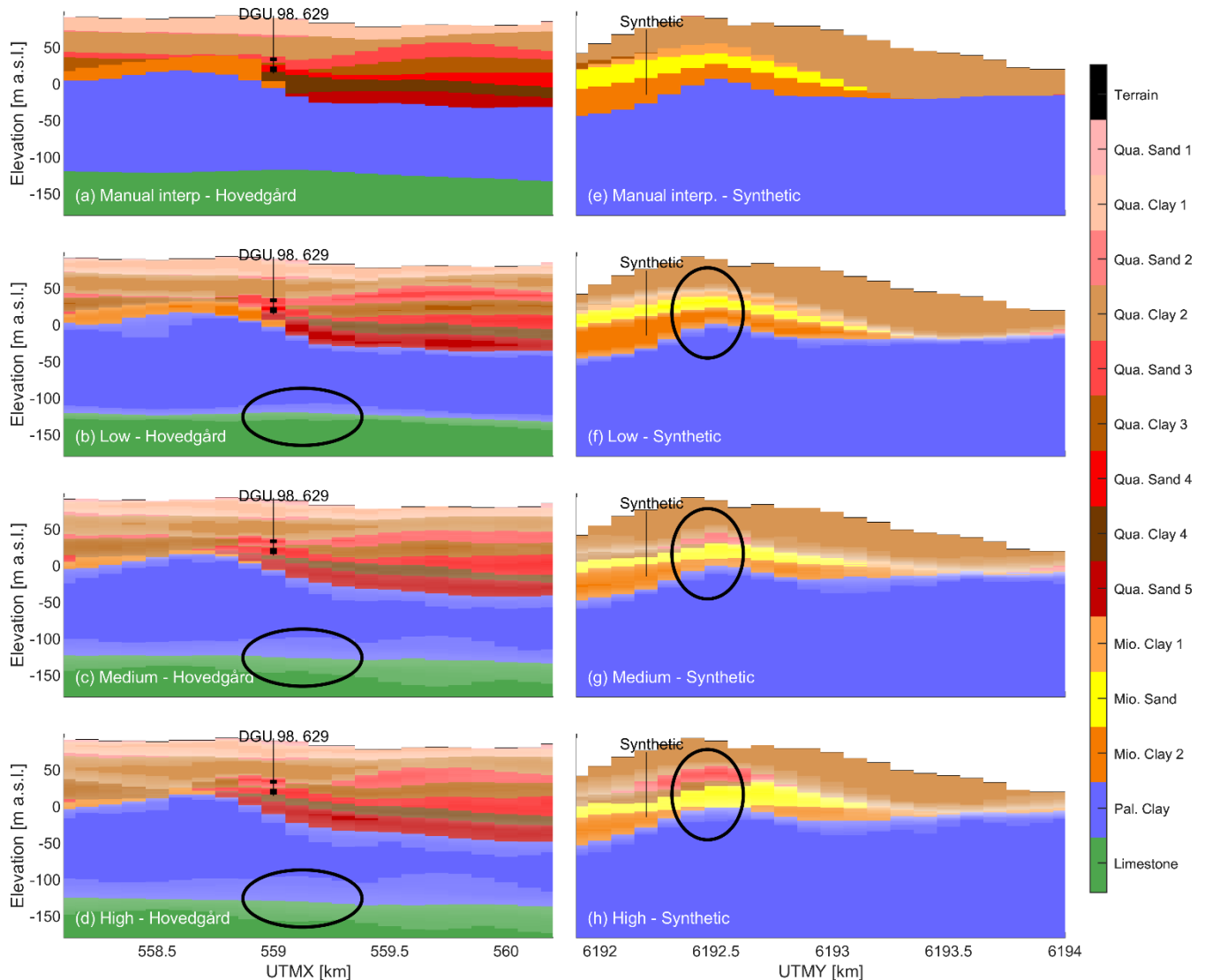
Figure 6: Two cross sections of summary statistics for the hydrostratigraphic model realizations at Hovedgård (a-d) and the synthetic (e-h) well field. Location of the profiles can be seen in Figure 1. Abstraction boreholes from the well fields are marked with a black line and the inlet filters marked with black rectangles. Note that the filter is missing on the cross sections at the synthetic borehole

350

355

In the real well fields (Højballegård and Hovedgård) (Figure 5 and Figure 6a-d), where the abundance of data and interpretation points is high, the difference in entropy is larger between the Low and Medium scenario than between the Medium and High scenario. This can be attributed to the lack of spatial freedom of the layer boundaries, being naturally constrained by the sheer number of interpretation points. In contrast, when the number of interpretation points is small, as is the case around the

360   synthetic well field (Figure 6d-f), both increasing and decreasing the uncertainty level has a significant impact on the resulting hydrostratigraphic realizations.

A slight change in mode can be observed between the three uncertainty scenarios (Figure 5 and Figure 6), which is a result of changing the smoothing in the LF-model, reflecting a lower information level. This difference is illustrated in regions with a low density of interpretation points, where the model may deviate significantly from the Manual Interpretation model. E.g., in

365   Figure 6h the average depiction of Quaternary sand deposits (red colors) is higher compared to Figure 6f-g. However, in areas with high interpretation point density, as seen around the well in Figure 5b-h, each uncertainty level has a similar mode model. In general, borehole information, where the uncertainty is rather low in all three scenarios, are easily identified for all three scenarios as vertical parts of the probabilistic model associated with low uncertainties near the layer boundaries of the model (e.g., white ellipse in Figure 5b-d). Despite the lowered uncertainty in these vertical sections, the trend of varying uncertainty

370   between the scenarios can also be spotted at these locations. All the above-mentioned observations are in accordance with expectations of the behavior of the model for the three uncertainty scenarios.

4.2 Groundwater model

In each of the three hydrostratigraphic uncertainty scenarios, the 50 hydrostratigraphic realizations are run with the same 200 groundwater parameter realizations in the groundwater model. In the following, the results of the groundwater models are

375   presented. In the Low, Medium and High uncertainty scenario, respectively, 7 %, 4 % and 3 % of the realizations did not converge and are therefore not included in the analysis. In section 4.1 it was observed that the realizations of the Low uncertainty scenario are not necessarily more like that of the original Manual Interpretation model than the realizations of High uncertainty scenario, which may explain the difference in the convergence rates. The convergence rate is likely influenced by the model grids that are unique for each realization as it follows the layer elevations. The model grid is thereby influenced by

380   the smoothing of the hydrostratigraphic model (Figure 3). The low smoothing of the Low uncertainty scenario allows larger changes in layer elevations than the high smoothing in the High uncertainty scenario. In areas where the layers are thin this may result in lack of lateral continuity between adjacent cells, which causes an inability to simulate flow between cells in the same layer. Further, at the synthetic well field, the water table falls below the screen top in 46 %, 6 % and 1 % of the

realizations respectively in the Low, Medium and High uncertainty scenario, which we will elaborate on in section 4.2.5. These
385   realizations are excluded from further analyses.

4.2.1 Ensemble performance

The performance of the model realizations in the three uncertainty scenarios is shown in Figure 7. The evaluated performance
metrics consist of root mean square error (RMS) and mean error (ME) of hydraulic head and river flow error. The grey area
illustrates ranges for the performance metrics outside the threshold values. In the Manual Interpretation model, thresholds have
390   been applied directly on the performance metrics. In the other uncertainty scenarios, the same parameters retained from the
Manual Interpretation model have been applied. The range for the performance metrics covered by the Manual Interpretation
model is therefore lowest, while it increases with uncertainty introduced in the uncertainty scenarios. It is shown that almost
90 % of the realizations (between the 5th and 95th percentile) are within the threshold values for the Low and Medium scenario
while it is a bit less for the High uncertainty scenario. The uncertainty of assuming that the same parameter sets are applicable
395   for the other hydrostratigraphic realizations is thereby illustrated. The simulations from the High uncertainty scenario have
larger ranges of variation for all performance criteria while the simulations from the Low uncertainty scenario have smaller
variations.
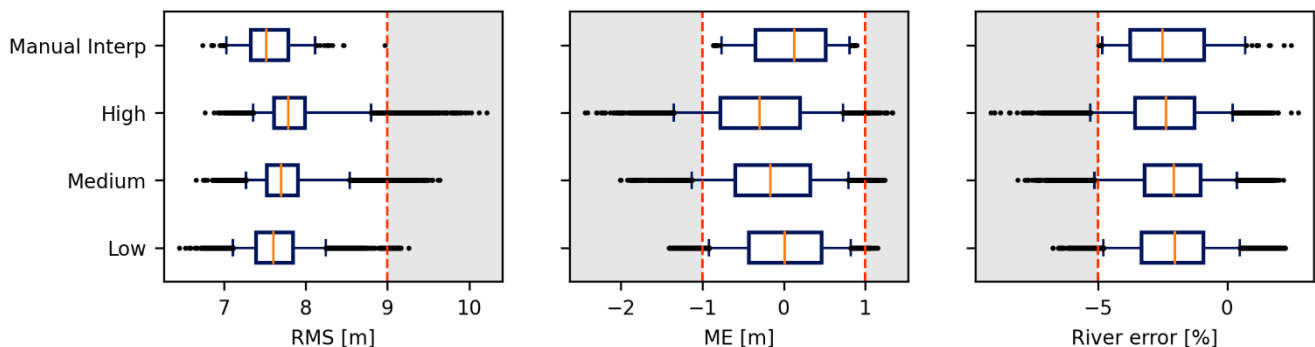
Figure 7: Performance in terms of Root Mean Square error (RMS) and Mean Error (ME) of hydraulic head and River error at the
400   **discharge station of the realizations within the three uncertainty scenarios Low, Medium and High and in the Manual Interpretation**
(Manual Interp) model. The boxes show the interquartile range between the 25th and 75th percentiles, while the whiskers mark the
5th and 95th percentiles. The median is indicated by the orange line. The Manual Interpretation scenario consists of 200 parameter
realizations, while the remaining scenarios consist of the same 200 parameter realizations combined with 50 hydrostratigraphic
realizations.

4.2.2 Predictions
405

A summary of the uncertainties of the groundwater model predictions is presented in Figure 8. The mean normalized standard
deviation of the median travel time and the mean normalized standard deviation of the capture zone area are shown on the x
and y axis, respectively. The mean standard deviation is a measure of the uncertainty within the predictions, which is

normalized to the predictions to enable a comparison between them. To obtain the normalized standard deviation, the standard
410   deviation of a parameter or a hydrostratigraphic realization (comprised of 50 different hydrostratigraphic realizations or 200
different parameter realizations, respectively) is divided by the ensemble mean prediction. The mean of the normalized
standard deviation of the parameter or hydrostratigraphic ensembles is then calculated. The predictions are marginalized on
the hydrostratigraphic realizations shown in orange or parameter realizations shown in blue. Further, the three well fields are
shown with different marker types and the three uncertainty scenarios are shown with different sizes of the markers in Figure
415   8.
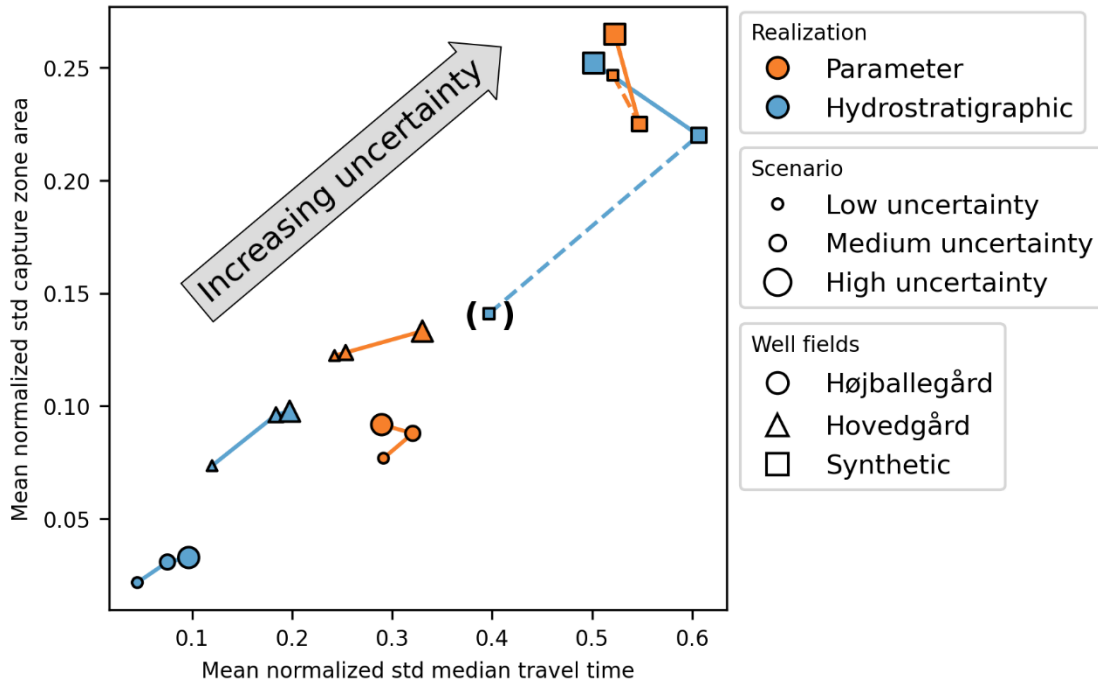
Figure 8: Mean normalized standard deviation of capture zone area and median travel time for all uncertainty scenarios (Low, Medium and High) and all well fields (Højballegård, Hovedgård and the Synthetic). The predictions have been marginalized on either parameter realizations (orange) or hydrostratigraphic realizations (blue). For the Synthetic well field in the low uncertainty
420   **scenario half of the hydrostratigraphic realizations had to be discarded and the predictions are therefore placed in a parenthesis.**

At least three effects can be observed in Figure 8. First, by comparing the parameter and hydrostratigraphic realizations
(different marker colors), the parameter uncertainty is shown to introduce a higher mean normalized standard deviation than
the hydrostratigraphic interpretation uncertainty. This is except for the synthetic well field, where the uncertainty introduced
from parameter and hydrostratigraphy to predictions becomes comparable. Second, by comparing results across well fields
425   (different marker types), the mean normalized standard deviation of Højballegård well field is lower than that of Hovedgård
well field which is again lower than that of the synthetic well field. Also, by comparing the results within the different
uncertainty scenarios, the higher uncertainty scenarios generally introduce a higher mean normalized standard deviation for

the predictions. Third, when comparing the results of the synthetic well field (square marker) to the other two well fields (circle and triangle marker), the difference in results of the hydrostratigraphic realizations between the uncertainty scenarios is larger in the synthetic well field. Further, the travel time variance does not increase from Medium to High uncertainty scenario, which is the case in the other two well fields. In the following, these three observations will be elaborated.

4.2.3 Hydrostratigraphic vs parameter realizations

To illustrate the influence of the hydrostratigraphic realizations on the capture zones, the capture zones to Højballegård and the synthetic well fields for randomly selected realizations are presented in Figure 9 and Figure 10. The capture zone areas are shown as probability maps where a value of 100 % signifies that particles placed in that cell are captured by the extraction well for all selected realizations. For each parameter realization (Figure 9b-e and Figure 10b-e), the results are based on 50 hydrostratigraphic realizations, while for each hydrostratigraphic realization (Figure 9g-j and Figure 10g-j), the results are based on 200 parameter realizations. As references, the capture zone area for the Manual Interpretation model (Figure 9f and Figure 10f) and for all realizations (Figure 9a and Figure 10a) are shown.

The results for Højballegård shown in Figure 9 represent the Low uncertainty scenario. The simulated capture zone areas for the parameter realizations are dominated by high probability values implying that the responses from the hydrostratigraphic realizations are similar. Correspondingly, the capture zone areas of the four hydrostratigraphic realizations are similar in extent and shape. On the other hand, the extent covered by the four parameter realizations is more diverse, illustrating a higher degree of disagreement between the parameter realizations. This is also illustrated in the four hydrostratigraphic realizations, where large parts of the capture zone area are dominated by low probabilities. The capture zone area of the synthetic well field in the High uncertainty scenario (Figure 10) is at the other end of the spectrum. Here, large parts of the capture zone area both in the hydrostratigraphic and parameter realizations have low probabilities. Correspondingly, the extent of the selected realizations covers different areas for both hydrostratigraphic and parameter realizations, indicating that both have a noticeable impact on the extent of the capture zone area.
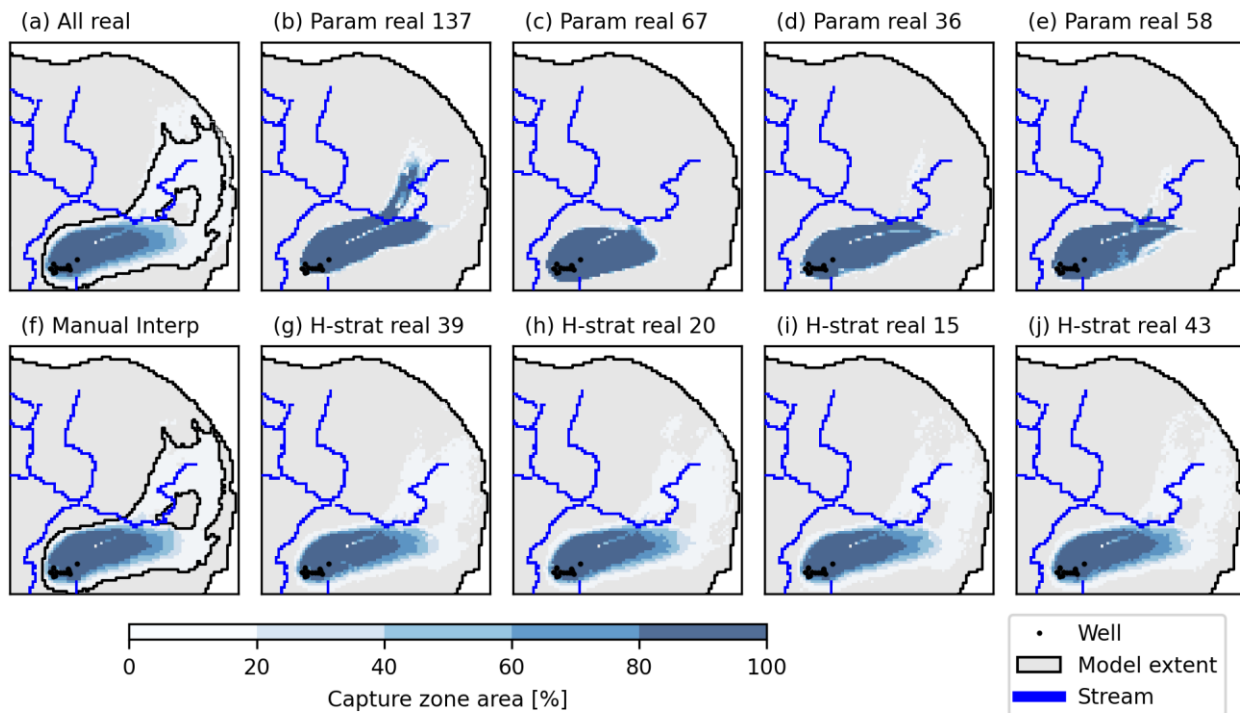
Figure 9: Capture zone area of the Højballegård well field in percentage of the realizations in the Low uncertainty scenario. The location of the plot is seen in Figure 1. Four parameter realizations (param real, b-e) and hydrostratigraphic realizations (h-strat real, g-j) have been randomly selected. In the hydrostratigraphic realizations as well as the Manual Interpretation model (f), the ensemble consists of 200 parameter realizations, while the ensemble consists of 50 hydrostratigraphic realizations in the parameter realizations. In the "All real" scenario, the ensemble consists of 50 hydrostratigraphic realizations and 200 parameter realizations.
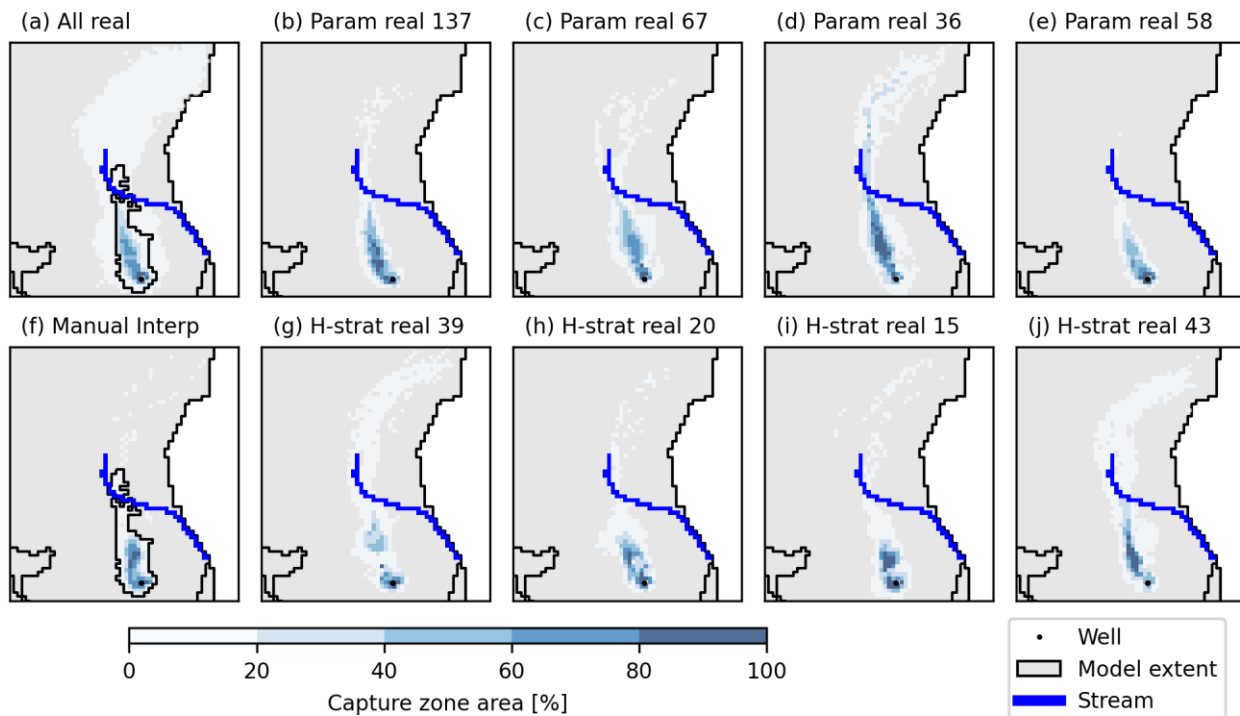
Figure 10: Capture zone area of the synthetic well field in percentage of the realizations in the High uncertainty scenario. The location of the plot is seen in Figure 1. Four parameter realizations (param real, b-e) and hydrostratigraphic realizations (h-strat real, g-j) have been randomly selected. In the hydrostratigraphic realizations as well as the Manual Interpretation model (f), the ensemble consists of 200 parameter realizations, while the ensemble consists of 50 hydrostratigraphic realizations in the parameter realizations. In the "All real" scenario, the ensemble consists of 50 hydrostratigraphic realizations and 200 parameter realizations.

4.2.4 Well fields

All capture zone areas in the High uncertainty scenario are illustrated in Figure 11. The results for the individual parameter realizations are shown in the columns of the matrices while the hydrostratigraphic realizations are shown in the rows. In the legend, two endmembers of the expected variation for a dominating parameter uncertainty and a dominating hydrostratigraphic uncertainty are shown. Red realization numbers correspond to the randomly selected realizations in Figure 10. The selected realization of Figure 9 is not marked here, as it was selected in the Low uncertainty scenario. For the Højballegård well field, the matrix has a dominating vertical structure, suggesting that the uncertainty is dominated by parameter uncertainty. In contrast, for the synthetic well field, the hydrostratigraphic realizations exert a stronger influence on the capture zone area, with no visually dominating row or column directions. The results for Hovedgård well field are in between the other two well fields.

Figure 2 illustrates the density of interpretation point categories at the three well fields. At Højballegård a high density of high certainty (category 1) interpretation points is placed around the well field. The density of interpretation points is lower in Hovedgård and lower still at the synthetic well field. However, as also evident in Figure 2, the hydrostratigraphy between the three well fields are different, i.e., Højballegård well field is characterized by large aquifers, while Hovedgård and the synthetic well field has thinner aquifers. We can therefore not isolate the effect that contributes to the highest impact of interpretation uncertainty at the synthetic well field and the lowest at Højballegård. We can only conclude that both the hydrostratigraphic structure and the certainty with which it has been described impacts the impact of interpretation uncertainty.
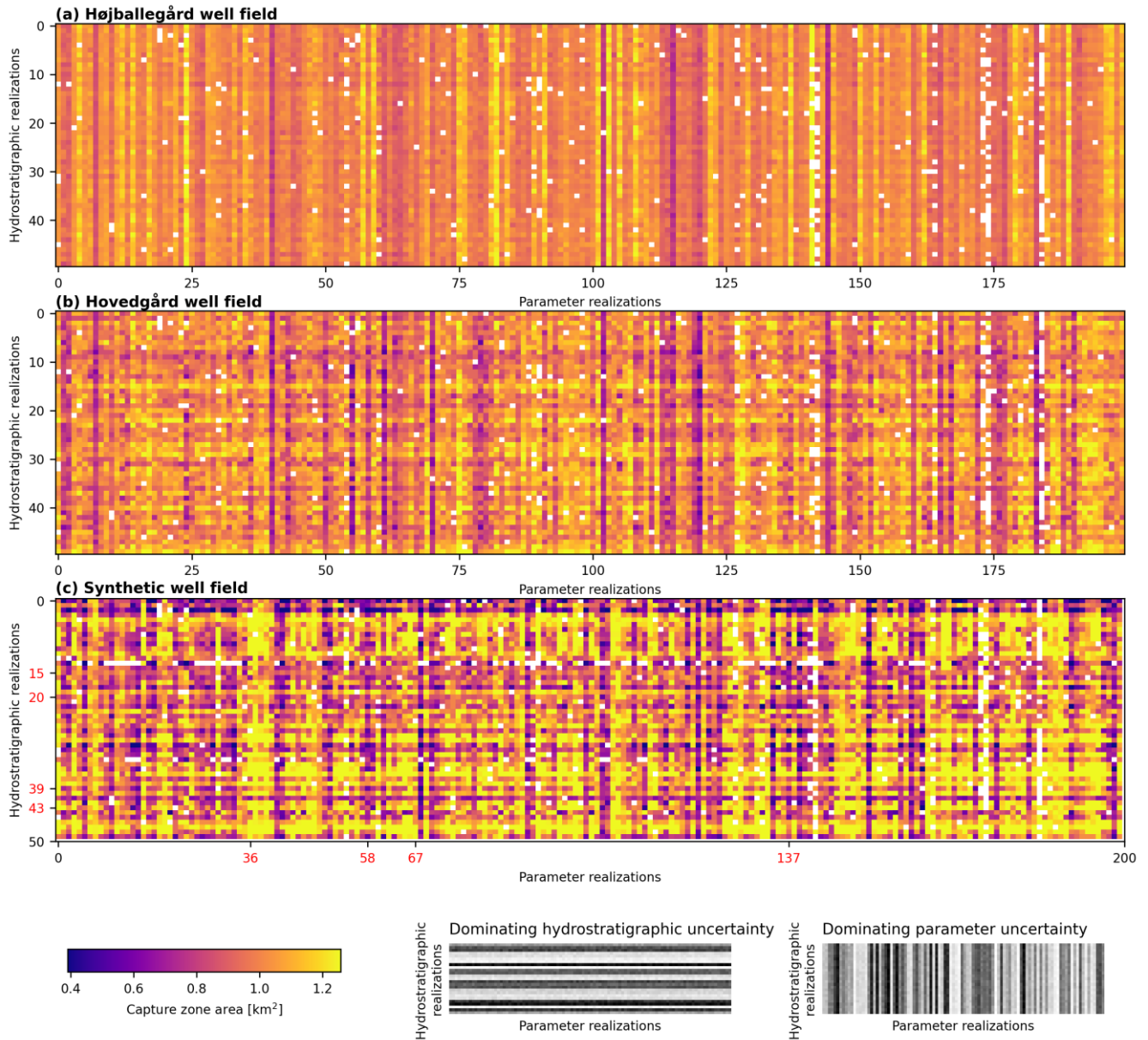
Figure 11: Simulated capture zone area to Højballegård, Hovedgård and the synthetic wellfields in the parameter realizations (columns) and hydrostratigraphic realizations (rows) in the High uncertainty scenario.

4.2.5 Synthetic well field

485 Figure 6d-f illustrates the impact of the uncertainty scenarios on the hydrostratigraphic models, where the yellow layer marks the Miocene sand from where the synthetic well is pumping. In the Low uncertainty scenario (Figure 6d), the Miocene layer

has a relatively high elevation compared to the Manual Interpretation model (Figure 6e) and other uncertainty scenarios. This is explained by a lack of interpretation points in the area to constrain the hydrostratigraphic model realizations. In half of the realizations, the elevation of the Miocene layer is above the water table (not shown), which means that predictions based on particle tracking cannot be calculated. The impact from the hydrostratigraphic realizations on the predictions in the Low uncertainty scenario is therefore underestimated. This explains the large difference in results between the uncertainty scenarios in the synthetic well field (Figure 8).

Also, from Figure 6 it can be observed that a red Quaternary sand layer appears in the Medium uncertainty scenario and becomes even more prominent in the High uncertainty scenario. Because of the relatively few interpretation points in this area (Figure 2), the stratigraphy changes between the uncertainty scenarios as the smoothing factor is changed. This may explain why the mean normalized standard deviation does not react the same way in response to the uncertainty scenarios in the synthetic well field as they do in the two real well fields (Figure 8).

5 Discussion

This study demonstrates a methodology to characterize interpretation uncertainty quickly and systematically of a manual interpretation model and to propagate the characterized interpretation uncertainty to a groundwater model. In the following, the results of the hydrostratigraphic and groundwater modelling will be discussed and will be translated into practical lessons.

5.1 Assessment of the hydrostratigraphic model

Expectations of the relative impact of the interpretation uncertainty were met in the results, i.e., interpretation uncertainty in areas of high certainty in the hydrostratigraphic model (Højballegård well field) was shown to have a relatively small impact on predictions, while the impact was more pronounced in areas of less geological certainty (synthetic well field). The result showed that scenarios with higher geological uncertainty generate higher variation of predictions. The results support the expected applicability of the method for incorporating geological interpretation uncertainty in groundwater models.

Nevertheless, the results from the synthetic well field were not as expected. The synthetic well field was shown to give rise to the largest predictive variance. As opposed to the real well fields, no borehole information from the well informs the geology in this well field. The modelled uncertainty in this area is therefore higher than what would be expected in most real-case well fields. It was shown that the layer sequence in the synthetic well field area is different from the original Manual Interpretation model in the hydrostratigraphic realizations (Figure 6), while the layer sequence remained at the other well fields. Thus, the characterized uncertainty within the hydrostratigraphic realizations at the synthetic well field had a different character than at the other well fields. To limit the risk of changes to the stratigraphy in areas with low density of interpretation points, the applied methodology could be extended with the following: 1) An expert knowledge filter could be applied to the resulting hydrostratigraphic realizations to ensure that realizations complied with a set of stratigraphic rules in specific areas, or 2) non-stationarity could be introduced such that the expected small-scale variability in the model could vary across the study area.

This would likely add more uncertainty in areas of high interpretation uncertainty, thus making synthetic wells behave more predictably.

5.2 Assessment of the groundwater model

The predictions by the groundwater models were calculated with a suite of parameters, which allowed the original interpretation model to replicate measured system behavior. To obtain the suite of parameters, the GLUE approach was applied, which is an informal Bayesian approach. According to Vrugt et al. (2009), the resulting parameter uncertainty from a GLUE approach is larger than that of a formal Bayesian approach. The parameter uncertainty may therefore be inflated compared to if a formal Bayesian approach had been applied. However, only a few parameters were involved in the analysis of the parameter uncertainty. The inclusion of more parameters in the uncertainty analysis would likely lead to an increase in estimated parameter uncertainty.

When applying the parameters from the original Manual Interpretation model, the replication of system behavior was shown to deteriorate slightly as more interpretation uncertainty was introduced in the uncertainty scenarios (Figure 7). This in turn gave rise to an increase in predictive variance between geological uncertainty scenarios (Figure 8). Thus, some inaccuracies must be anticipated assuming that the posterior parameter range from the interpretation model is applicable to other hydrostratigraphic realizations. However, this assumption was deemed necessary to make the problem computationally tractable, as the alternative is to make a calibration of all hydrostratigraphic realizations. Another alternative is simulation-based learning to obtain the posterior distribution for the different scenarios (Hermans et al., 2023; Thibaut et al., 2021).

As only one out of many possible parameter uncertainty estimation methods were applied and the uniqueness of the study area in terms of geology and data density considered, no general conclusions will be made about the relative importance of geological interpretation uncertainty and parameter uncertainty. However, in this study a limited influence of the interpretation uncertainty compared to parameter uncertainty for predictions of capture zone area and median travel time was found in a geologically well-defined area with thick aquifers. In a geologically poorly defined area with thin aquifers, the influence of interpretation uncertainty and parameter uncertainty became comparable. Other studies testing the uncertainty of the hydrostratigraphic model have concluded that the model structure is dominating compared to parameter uncertainty (e.g. Højberg and Refsgaard, 2005). The difference is that in this study, only the interpretation uncertainty within a given conceptual model has been characterized and not the conceptual uncertainty itself. Given that the presented level of uncertainty is a fair representation, our results thereby confirm existing evidence (e.g. Neuman and Wierenga, 2003; Rojas et al., 2010) that the choice of the conceptual model imposes a far greater impact on to the groundwater model predictions than the interpretation uncertainty within the manually interpreted model.

5.3 Lessons of practical nature

This study's generalizability is restricted by the specific characteristics of the study area. Egebjerg is geologically very complex with several generations of buried valleys crossing each other, glaciotectonic disturbed layers and a deep fault zone disturbing

550   the layers. So even though the area is relatively data dense, and a well-defined conceptual model has been developed, the hydrostratigraphic connections between the layers are uncertain due to the geological complexity of the area. It has therefore been questioned whether the area could be accurately represented by a simple layer model (Enemark et al., 2022). This geological complexity of the area also results in relatively poor performance of the groundwater model with the best root mean square error around 7 m, indicating potential flaws in the conceptual understanding.

555   For practical purposes, at least in Denmark, a buffer-zone is often added to the capture zone area simulated by a groundwater model based on a single hydrostratigraphic model to take account of unspecified uncertainty (Iversen et al., 2009). Two problems relate to the application of the buffer-zone approach: 1) The necessary width of the buffer-zone is based on a subjective assessment of the uncertainty in the area, and 2) A simple buffer-zone cannot capture spatial trends in the capture zone area that are not radially expanding. From a management point of view, this is not ideal as areas not part of the real

560   capture zone may be included, while other relevant areas may be excluded. However, in a case where the impact of interpretation uncertainty is low (Figure 9a), the buffer approach with e.g. a 200 m buffer around the Manual Interpretation model from Figure 9f appears to be sufficient in order to capture the uncertainty in the capture zone area The approach presented in this study, offers an alternative to the buffer-zone approach at the expense of an increase in computational time, but with the benefit of higher certainty that a more realistic capture zone area has been obtained.

565   From an interpretation point of view, our results indicate limited difference between the Low, Medium and High uncertainty scenario. This suggests that the geological interpreter can feel more at ease during interpretation as to whether the exact location of the layer boundary has been identified correctly. The impact of interpretation uncertainty within a conceptual model would be highly dependent on the geological structures and complexity implying that precise interpretations are more needed in areas with thin aquifers (such as the area around the synthetic well field) than in areas with thick and laterally extensive aquifers as

570   around Højballegård well field. The scale of the influence is also dependent on the data density and quality in the area. As the Egebjerg study area is a data dense area, future work should include areas closer to the average and even low data availability, where the influence of interpretation uncertainty will likely be higher.

6 Conclusion

While the interpretation uncertainty of a deterministic hydrostratigraphic model is a known accessory, it has until recently

575   been difficult to propagate these uncertainties from the hydrostratigraphic model to a groundwater model. This study has shown an approach to systematically characterize the impact of hydrostratigraphic model interpretation uncertainties in groundwater modeling. The applied groundwater model was a full 3D model in which the vertical discretization follows the

hydrostratigraphic units. Results showed that it is possible to represent the interpretation uncertainty in areas with low geological uncertainty containing thick, large aquifers with a buffer zone, but in areas of high geological uncertainty and thinner, smaller aquifers, the interpretation uncertainty could be just as significant as parameter uncertainty. This study confirms that if the uncertainty of the conceptual model is small, the small-scale variability within the conceptual model is of less importance. This suggests that, in a geological modeling exercise, it is more worthwhile to invest time in developing a clearly defined conceptual model or even better, multiple conceptual models. The actual interpretation of data using the conceptual model(s) is of less importance for the groundwater model predictions.

7 Author contribution

RBM has overseen modeling different scenarios of geological uncertainties. TE has performed groundwater modeling and subsequent analysis. AH initiated the original idea. PS, LTA, IM and AH provided valuable insights into geological uncertainties and interpretations, while TS, KHJ and JK assisted in the analysis of the groundwater data. All authors contributed to the interpretation, analysis, and discussion of the results. RBM, AH and TE prepared the first draft of the manuscript with contributions from all co-authors.

8 Competing interests

The authors declare that they have no conflict of interest.

9 Acknowledgements

This study was primarily carried out as part of the Geoconcept project, funded by GeoCenter Denmark, with the aim to assess the impact of hydrostratigraphic modeling concepts on groundwater flow and transport modeling. The authors would also like to acknowledge Innovation Fund Denmark for funding RESPROB (Grant Number 7017-00160B) that enabled the work on interpretation uncertainties. The quality of this manuscript was improved by the review of Thomas Hermans, Mark Bierkens and one anonymous reviewer.

10 References

Andersen, L.T., Sandersen, P.B.E., 2020. GeoConcept – 3D hydrostratigrafisk lagmodel for Egebjerg (GEUS report 2020/59). https://doi.org/10.22008/gpub/34556

Bakker, M., Post, V., Langevin, C.D., Hughes, J.D., White, J.T., Starn, J.J., Fienen, M.N., 2016. Scripting MODFLOW Model Development Using Python and FloPy. Groundwater 54. https://doi.org/10.1111/gwat.12413

Barfod, A.A.S., Vilhelmsen, T.N., Jørgensen, F., Christiansen, A. V., Hyer, A.S., Straubhaar, J., Møller, I., 2018. Contributions to uncertainty related to hydrostratigraphic modeling using multiple-point statistics. Hydrol. Earth Syst. Sci. 22, 5485–5508. https://doi.org/10.5194/hess-22-5485-2018

Benoit, N., Marcotte, D., Molson, J., 2021. Stochastic correlated hydraulic conductivity tensor calibration using gradual deformation. J. Hydrol. 594. https://doi.org/https://doi.org/10.1016/j.jhydrol.2020.125880.

Beven, K.J., Binley, A., 1992. The future of distributed models: Model calibration and uncertainty prediction. Hydrol. Process. 6, 279–298. https://doi.org/10.1002/hyp.3360060305

Christiansen, A. V., Auken, E., 2012. A global measure for depth of investigation. Geophysics 77. https://doi.org/https://doi.org/10.1190/geo2011-0393.1

Curtis, A., 2012. The science of subjectivity. Geology 40, 95–96. https://doi.org/10.1130/focus012012.1

Danielsen, J.E., Auken, E., Jørgensen, F., Søndergaard, V.H., Sørensen, K.I., 2003. The application of the transient electromagnetic method in hydrogeophysical surveys. Jounral Appl. Geophys. 53, 181–198.

Enemark, T., Andersen, L.T., Høyer, A.-S., Jensen, K.H., Kidmose, J., Sandersen, P.B.E., Sonnenborg, T.O., 2022. The influence of layer and voxel geological modelling strategy on groundwater modelling results. Hydrogeol. J. 30, 617–635. https://doi.org/https://doi.org/10.1007/s10040-021-02442-9

Feyen, L., Caers, J., 2006. Quantifying geological uncertainty for flow and transport modeling in multi-modal heterogeneous formations. Adv. Water Resour. 29, 912–929. https://doi.org/10.1016/j.advwatres.2005.08.002

Hansen, B., Sonnenborg, T.O., Møller, I., Bernth, J.D., Høyer, A.S., Rasmussen, P., Sandersen, P.B.E., Jørgensen, F., 2016. Nitrate vulnerability assessment of aquifers. Environ. Earth Sci. 75. https://doi.org/10.1007/s12665-016-5767-2

Harrar, W.G., Sonnenborg, T.O., Henriksen, H.J., 2003. Capture zone, travel time, and solute-transport predictions using inverse modeling and different geological models. Hydrogeol. J. 11, 536–548. https://doi.org/10.1007/s10040-003-0276-2

He, X., Sonnenborg, T.O., Jørgensen, F., Høyer, A.S., Møller, R.R., Jensen, K.H., 2013. Analyzing the effects of geological and parameter uncertainty on prediction of groundwater head and travel time. Hydrol. Earth Syst. Sci. 17, 3245–3260. https://doi.org/10.5194/hess-17-3245-2013

Henriksen, H.J., Troldborg, L., Sonnenborg, T., Højberg, A.L., Stisen, S., Kidmose, J.B., Refsgaard, J.C., 2017. Hydrologisk geovejledning: God praksis i hydrologisk modellering (In Danis.

Hermans, T., Goderniaux, P., Jougnot, D., Fleckenstein, J.H., Brunner, P., Nguyen, F., Linde, N., Huisman, J.A., Bour, O., Lopez Alvis, J., Hoffmann, R., Palacios, A., Cooke, A.K., Pardo-Álvarez, Á., Blazevic, L., Pouladi, B., Haruzi, P., Fernandez Visentini, A., Nogueira, G.E.H., Tirado-Conde, J., Looms, M.C., Kenshilikova, M., Davy, P., Le Borgne, T., 2023. Advancing measurements and representations of subsurface heterogeneity and dynamic processes: Towards 4D hydrogeology. Hydrol. Earth Syst. Sci. 27, 255–287. https://doi.org/10.5194/hess-27-255-2023

Hills, R.G., Wierenga, P.J., 1994. INTRAVAL Phase II Model Testing at the Las Cruces Trench Site. NUREG/CR-6063.

Højberg, A.L., Refsgaard, J.C., 2005. Model uncertainty - parameter uncertainty versus conceptual models. Water Sci.

Technol. 52, 177–186.

Høyer, A.-S., Jørgensen, F., Lykke-Andersen, H. Christiansen, A.V., 2014. Iterative modelling of AEM data based on a priori information from seismic and borehole data. Near Surf. Geophys. 12, 635–650.

Høyer, A.-S., Jørgensen, F., Sandersen, P.B.E., Viezzoli, A., Møller, I., 2015. 3D geological modelling of a complex buried-valley network delineated from borehole and AEM data. J. Appl. Geophys. 122, 94–102. https://doi.org/10.1016/j.jappgeo.2015.09.004

Høyer, A.-S., Klint, K.E.S., Fiandaca, G., Maurya, P.K., Christiansen, A.V., Balbarini, N., Bjerg, P.L., Hansen, T.B., Møller, I., 2019. Development of a high-resolution 3D geological model for landfill leachate risk assessment. Eng. Geol. 249, 45–59. https://doi.org/10.1016/j.enggeo.2018.12.015

Høyer, A.-S., Sandersen, P.B.E., Mortensen, M.H., Andersen, L.T., Møller, I., 2023. Uncertainty Assessments in 3D Geological Modelling of Complex Unconsolidated Sediments – with Emphasis on Handling Subjectivity in the Entire Workflow. https://doi.org/10.2139/ssrn.4444386

Høyer, A.-S., Vignoli, G., Hansen, T.M., Vu, L.T., Keefer, D.A., Jørgensen, F., 2017. Multiple-point statistical simulation for hydrogeological models: 3-D training image development and conditioning strategies. Hydrol. Earth Syst. Sci. 21, 6069–6089. https://doi.org/10.5194/hess-21-6069-2017

Huysmans, M., Dassargues, A., 2009. Application of multiple-point geostatistics on modelling groundwater flow and transport in a cross-bedded aquifer (Belgium). Hydrogeol. J. 17, 1901–1911. https://doi.org/10.1007/s10040-009-0495-2

I-GIS, 2023. GeoScene3D [WWW Document]. URL http://www.geoscene3d.com (accessed 3.16.23).

Iversen, C.H., Lauritsen, L.U., Nyholm, T., Kürstein, J., 2009. Geo-Vejledning 2: Udpegning af indvindings- og grundvandsdannende oplande (Del 1) - Vejledning i oplandsberegninger i forbindelse med den nationale grundvandskortlægning (In Danish). GEUS Special Publication, Copenhagen, Denmark.

Jørgensen, F., Møller, R.R., Nebel, L., Jensen, N.P., Christiansen, A.V., Sandersen, P.B.E., 2013. A method for cognitive 3D geological voxel modelling of AEM data. Bull. Eng. Geol. Environ. 72, 421–432. https://doi.org/10.1007/s10064-013-0487-2

Jørgensen, F., Møller, R.R., Sandersen, P.B.E., Nebel, L., 2010. 3-D Geological Modelling of the Egebjerg Area, Denmark, Based on Hydrogeophysical Data. Geol. Surv. Denmark Greenl. Bull. 20, 27–30. https://doi.org/10.34194/geusb.v20.4892

Journel, A., Zhang, T., 2006. The necessity of a multiple-point prior model. Math. Geol. 38, 591–610. https://doi.org/10.1007/s11004-006-9031-2

Li, Z., Wang, X., Wang, H., Liang, R.Y., 2016. Quantifying stratigraphic uncertainties by stochastic simulation techniques based on Markov random field. Eng. Geol. 201, 106–122.

Madsen, R.B., Høyer, A.S., Andersen, L.T., Møller, I., Hansen, T.M., 2022. Geology-driven modeling: A new probabilistic approach for incorporating uncertain geological interpretations in 3D geological modeling. Eng. Geol. 309. https://doi.org/10.1016/j.enggeo.2022.106833

Madsen, R.B., Kim, H., Kallesøe, A.J., Sandersen, P.B.E., Vilhelmsen, T.N., Hansen, T.M., Christiansen, A.V., Møller, I., Hansen, B., 2021. 3D multiple point geostatistical simulation of joint subsurface redox and geological architectures. Hydrol. Earth Syst. Sci. 25, 2759–2787. https://doi.org/https://doi.org/10.5194/hess-2020-444.

675   Mariethoz, G., Caers, J., 2015. Multiple-point geostatistics: Stochastic modeling with training images, 1st ed. John Wiley & Sons.

Moore, C., Doherty, J., 2005. Role of the calibration process in reducing model predictive error. Water Resour. Res. 41, 1–14. https://doi.org/10.1029/2004WR003501

Neuman, S.P., Wierenga, P.J., 2003. A Comprehensive Strategy of Hydrogeologic Modeling and Uncertainty Analysis for

680   Nuclear Facilities and Sites. NUREG/CR-6805 311.

Niswonger, R.G., Panday, S., Motomu, I., 2011. MODFLOW-NWT , A Newton Formulation for MODFLOW-2005. USGS reports 44.

Poeter, E., Anderson, D., 2005. Multimodel ranking and inference in ground water modeling. Ground Water 43, 597–605. https://doi.org/10.1111/j.1745-6584.2005.0061.x

685   Refsgaard, J.C., Christensen, S., Sonnenborg, T.O., Seifert, D., Højberg, A.L., Troldborg, L., 2012. Review of strategies for handling geological uncertainty in groundwater flow and transport modeling. Adv. Water Resour. 36, 36–50. https://doi.org/10.1016/j.advwatres.2011.04.006

Refsgaard, J.C., van der Sluijs, J.P., Brown, J., van der Keur, P., 2006. A framework for dealing with uncertainty due to model structure error. Adv. Water Resour. 29, 1586–1597. https://doi.org/10.1016/j.advwatres.2005.11.013

690   Rojas, R.M., Batelaan, O., Feyen, L., Dassargues, A., 2010. Assessment of conceptual model uncertainty for the regional aquifer Pampa del Tamarugal – North Chile. Hydrol. Earth Syst. Sci. Discuss. 6, 5881–5935. https://doi.org/10.5194/hessd-6-5881-2009

Royse, K.R., 2010. Combining numerical and cognitive 3D modelling approaches in order to determine the structure of the Chalk in the London Basin. Comput. Geosci. 36, 500–511. https://doi.org/10.1016/j.cageo.2009.10.001

695   Sandersen, P.B.E., 2008. Uncertainty assessment of geological models - A qualitative approach. IAHS-AISH Publ. 345–349.

Sandersen, P.B.E., Jørgensen, F., 2016. Kortlægning af begravede dale i Danmark (Mapping of Buried Valleys in Denmark), Opdatering 2015 (Update 2015). Volumes 1 & 2 (In Danish). GEUS Special Publication, Copenhagen, Denmark.

Sandersen, P.B.E., Jørgensen, F., Kallesøe, A.J., Møller, I., 2018. Geo-vejledning 2018/1 - Opstilling af geologiske modeller til grundvandsmodellering (In Danish). GEUS Special Publication, Copenhagen, Denmark.

700   Seifert, D., Sonnenborg, T.O., Refsgaard, J.C., Højberg, A.L., Troldborg, L., 2012. Assessment of hydrological model predictive ability given multiple conceptual geological models. Water Resour. Res. 48, 1–16. https://doi.org/10.1029/2011WR011149

Stafleu, J., Maljers, D., Gunnink, J.L., Menkovic, A., Busschers, F.S., 2011. 3D modelling of the shallow subsurface of Zeeland, the Netherlands. Geol. en Mijnbouw/Netherlands J. Geosci. 90, 293–310.

705   https://doi.org/10.1017/S0016774600000597

Thibaut, R., Laloy, E., Hermans, T., 2021. A new framework for experimental design using Bayesian Evidential Learning: The case of wellhead protection area. J. Hydrol. 603, 126903. https://doi.org/10.1016/j.jhydrol.2021.126903

Troldborg, L., Ondracek, M., Koch, J., Kidmose, J., Refsgaard, J.C., 2021. Quantifying stratigraphic uncertainty in groundwater modelling for infrastructure design. Hydrogeol. J. 29, 1075–1089. https://doi.org/10.1007/s10040-021-02303-5

Troldborg, L., Refsgaard, J.C., Jensen, K.H., Engesgaard, P., 2007. The importance of alternative conceptual models for simulation of concentrations in a multi-aquifer system. Hydrogeol. J. 15, 843–860. https://doi.org/10.1007/s10040-007-0192-y

Viezzoli, A., Jørgensen, F., Sørensen, C., 2013. Flawed Processing of Airborne EM Data Affecting Hydrogeological Interpretation. Groundwater 51, 191–202. https://doi.org/10.1111/j.1745-6584.2012.00958.x

Vignoli, G., Fiandaca, G., Christiansen, A.V., Kirkegaard, C., Auken, E., 2015. Sharp spatially constrained inversion with applications to transient electromagnetic data. Geophys. Prospect. 63, 243–255.

Vrugt, J.A., ter Braak, C.J.F., Gupta, H. V., Robinson, B.A., 2009. Equifinality of formal (DREAM) and informal (GLUE) Bayesian approaches in hydrologic modeling? Stoch. Environ. Res. Risk Assess. 23, 1011–1026. https://doi.org/10.1007/s00477-008-0274-y

Wellmann, F., Caumon, G., 2018. 3-D Structural Geological Models: Concepts, Methods, and Uncertainties. Adv. Geophys. 59, 1-121-.

Zhang, J.Z., Huang, H.W., Zhang, D.M., Phoon, K.K., Liu, Z.Q., Tang, C., 2021. Quantitative evaluation of geological uncertainty and its influence on tunnel structural performance using improved coupled Markov chain. Acta Geotech. 16, 3709–3724.